Cytometry Part A 59A:203–209 (2004)

Deformability-Based Flow Cytometry

Bryan Lincoln,[1] Harold M. Erickson,[2] Stefan Schinkinger,[1] Falk Wottawah,[1] Daniel Mitchell,[3] Sydney Ulvick,[3] Curt Bilby,[3] and Jochen Guck[1]*

[1]Institute for Soft Matter Physics, University of Leipzig, Leipzig, Germany
[2]Tom C. Mathews Familial Melanoma Research Clinic, Huntsman Cancer Institute, Salt Lake City, Utah
[3]Evacyte Corporation, Austin, Texas

Received 8 December 2003; Revision Received 27 February 2004; Accepted 1 March 2004

Background: Elasticity of cells is determined by their cytoskeleton. Changes in cellular function are reflected in the amount of cytoskeletal proteins and their associated networks. Drastic examples are diseases such as cancer, in which the altered cytoskeleton is even diagnostic. This connection between cellular function and cytoskeletal mechanical properties suggests using the deformability of cells as a novel inherent cell marker.
Methods: The optical stretcher is a new laser tool capable of measuring cellular deformability. A unique feature of this deformation technique is its potential for high throughput, with the incorporation of a microfluidic delivery of cells.
Results: Rudimentary implementation of the microfluidic optical stretcher has been used to measure optical deformability of several normal and cancerous cell types. A drastic difference has been seen between the response of red blood cells and polymorphonuclear cells for a given optically induced stress. MCF-10, MCF-7, and modMCF-7 cells were also measured, showing that while cancer cells stretched significantly more (five times) than normal cells, optical deformability could even be used to distinguish metastatic cancer cells from nonmetastatic cancer cells. This trimodal distribution was apparent after measuring a mere 83 cells, which shows optical deformability to be a highly regulated cell marker.
Conclusions: Preliminary work suggests a deformability-based cell sorter similar to current fluorescence-based flow cytometry without the need for specific labeling. This could be used for the diagnosis of all diseases, and the investigation of all cellular processes, that affect the cytoskeleton. © 2004 Wiley-Liss, Inc.

Key terms: optical stretcher; cell marker; diagnosis; microfluidics; breast cancer; metastasis; stem cells; RBC; PMN; optical deformability

Flow cytometers can measure and sort cells based on their various distinguishable features. Apart from size and surface characteristics found by analyzing forward- and side-scattered light, flow cytometry conventionally relies on the use of fluorescent cell markers (1). With the advent of a new laser tool, the optical stretcher (2,3), we exploit cellular deformability, a novel inherent cell marker capable of adding a completely new dimension to this field.

For eukaryotic cells, the mechanical properties depend mainly on the cytoskeleton, an intricate polymeric network that spans the whole interior of the cell (4). An active, highly nonlinear, dynamic system far away from thermal equilibrium, the cytoskeleton requires significant energy to maintain its structure as well as to carry out important cellular tasks (4). Actin filaments, semiflexible polymers that are involved in cell motility and division, form an actin cortex that is the key component of their elastic and viscous response. Microtubules are stiff rods that act as intracellular highways and are mostly responsible for ribosomal and vesicle transport and the separation of chromosomes. Intermediate filaments are flexible polymers that offer cell strength at large deformations (5,6). These three polymeric components, whose interplay is already apparent because they all contribute in some way to mitosis and mechanotransduction (7,8), combine to form a heterogeneous soft-matter structure.

This polymeric structure will vary depending on a cell's function, one illustrative example of which is a malig-

Contract grant sponsors: Wolfgang-Paul Prize from the Humboldt Foundation; Evacyte Corporation, Austin, Texas.
*Correspondence to: Jochen Guck, University of Leipzig, Linnéstr. 5, 04103 Leipzig, Germany.
E-mail: jguck@physik.uni-leipzig.de
Published online 17 May 2004 in Wiley InterScience (www.interscience.wiley.com).
DOI: 10.1002/cyto.a.20050

nantly transformed cell. Proteomic and microscopic techniques have shown that the available polymeric network undergoes a significant restructuring during this process, changing from an ordered, rigid structure to a more irregular and malleable state, including an overall reduced amount of accessory proteins and cytoskeletal polymers (9–11). These alterations are intuitive, as malignant cells are known for replication and motility, neither of which relies on a rigid cytoskeleton.

Similar cytoskeletal alterations are found during the normal development of cells. Stem cells are immortal and replicating "master cells" that spawn all differentiated cell types. Many signaling pathways involved in the differentiation of stem cells, which are being discovered, involve proteins that are either directly or indirectly involved in the organization and regulation of the cytoskeleton (8,12). The differences found between differentiated and undifferentiated cells included changes in the absolute amount of the cytoskeletal proteins, cytoskeletal polarization, and thickness of the cortical actin ring (13,14).

All these findings about cytoskeletal changes consist of molecular details that cannot be easily measured directly for identifying the function of a single cell. The combined effect of these changes in cytoskeletal content and structure, however, should also be reflected in the overall mechanical properties of the cell, which would mean that measuring a cell's rigidity may be viewed as a new biological marker sensitive to cell function. The relationship between structural content and elasticity is described by polymer physics; one very relevant result is that the shear modulus of a solution of actin filaments scales with the actin concentration raised to a power of 2.2 (5). This means that even small molecular changes may be strongly enhanced in the overall elasticity measured in the cell.

There have been past direct experimental attempts that point toward this connection between deformability and cell function, but the measurement techniques have been limited in a variety of ways. These include mechanical contact of the probe causing adhesion and active cellular response, special preparation and handling leading to measurement artifacts, and, most importantly, low throughput resulting in poor statistics. The historically prevalent technique for measuring single cells in detail has been micropipette aspiration (15), which has found a 50% reduction in elasticity and a 30% reduction in the viscous response of malignantly transformed fibroblasts as compared to their normal counterparts (16). Here, a micropipette is carefully placed onto the surface of a cell. By applying a negative pressure, a portion of the cell is aspirated into the pipette in inverse proportion to its rigidity. More recently, atomic force microscopy (AFM) has been used for the determination of cellular rigidity (17,18), including the investigation of normal human bladder endothelial cell lines and complimentary cancerous cell lines, for which it was found that their rigidity differed by an order of magnitude (19). Other notable techniques include cell pokers (20), microplate manipulation (21), microbead rheology (22), and the manipulation of beads attached to cells with optical tweezers (23).

There are some techniques that can assess the deformability of many cells simultaneously, such as cell-pellet rheology (24) or ektacytometry (25). Both techniques share the problem of performing ensemble measurements, in which the presence of a few very different cells goes unnoticed and is lost in the noise. Even if detectable, a separation of a few cells with these techniques would be impossible.

These various methods have sufficiently indicated a strong correlation between elasticity and function of cells and suggest using cellular deformability as a general inherent cell marker. What has been missing is a technique capable of measuring a large number of individual cells in a short period of time. The microfluidic optical stretcher is the first experimental tool that is able to do this using the viscoelastic properties of individual cells. In addition to its quickness, it has the added advantage of being noninvasive; the cells need no marker, or any sort of mechanical attachment.

MATERIALS AND METHODS

The Microfluidic Optical Stretcher

The optical stretcher (Fig. 1) utilizes two divergent counter-propagating, fiber-optically aligned laser beams, which act as a stable trap at low laser intensities (2,26). At higher intensities, measurable deformations are observed due to forces induced at the surface by momentum transfer (Fig. 2) (2). This enables a suspended cell to be trapped, and subsequently to undergo a light-intensity- and duration-controlled deformation experiment, using the same beams that compose the trap.

For two identical, opposing, light beams, the cell becomes trapped along the beam axis at the midpoint between the two sources. Its stability comes from the restoring force of this configuration; any cell displaced along the beams will feel a net scattering force directed back toward the midpoint, while any cell displaced away from the main axis will feel a gradient force toward the more intense center of the beams' Gaussian profiles (3). The fact that the optical stretcher can automatically trap and center cells is of paramount importance for high throughput.

While a cell is in the trap, the light passing through it exerts a stress normal to the surface and toward the less optically dense surrounding medium (2). The maximum occurs at the two points where the surface encounters the beam axis, while the minimum occurs in a line around the middle of the cell, where the surface is perpendicular to the direction of light propagation and the magnitude of the stress is zero. If the stress is high enough to deform the cytoskeleton, the cell will be stretched out along the beam axis. The stress profile can be calculated for a Gaussian beam incident on a spherical object using ray optics (Fig. 3). In this approximation the stress depends on the laser power, the ratio of the beam and cell radii, and the index of refraction of both the cell and the surrounding medium. The power generally ranges from trapping powers as low as 5 mW for some cell types up to a maximal stretching power approaching 2 W in each beam. A wavelength of

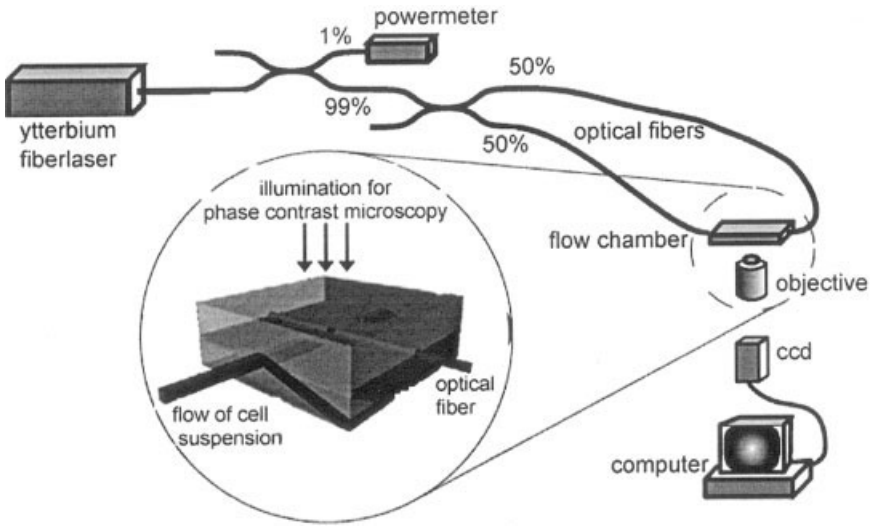

FIG. 1. Schematic diagram of the microfluidic optical stretcher. An optical fiber connected to a fiber laser is split evenly into two fibers, each with one-half of the initial beam. These fibers are aligned opposing each other and within a microfluidic chamber (see inset). Data is gathered using phase contrast microscopy.

1,064 nm is used in order to minimize any cell damage caused by the absorption of laser energy by the cell (3). The beams undergo diffraction-limited divergence, so their radii in the trap region are controlled by the distance of the two sources. The index of refraction of the medium can be measured directly, while that of the cell can be determined using index matching (3).

The peak force on a cell trapped in 1-W laser beams is in the 200–500 pN (piconewton) range. This is enough to deform most cells, while the divergence of the beam ensures that the cells are not damaged despite the relatively high powers used (27).

Microfluidic Delivery

Different cells of the same cell type will not be identical, meaning that one would expect to measure a distribution of values for a certain cell type. To learn what this distribution is (to reasonable accuracy) required the measurement of more than a few cells, necessitating the development of a delivery system that enables a high throughput of individual cells into and out of the trap (Fig. 4).

This was achieved with two different configurations. One setup used a microfabricated polydimethylsiloxane (PDMS) structure that aligns optical fibers perpendicular to a flow channel on the order of about 80–100 μm wide and tall. By molding the PDMS over a variety of photoresist structures, the dimensions of the flow channel could easily be varied from one setup to the next, and extra channels could be incorporated for possible sorting applications. The second, simpler setup used a microcapillary tube as the flow channel, with externally aligned fibers.

Size-Corrected Percent Stretch

To measure each cell's response to the optically induced stresses, video phase-contrast microscopy was used. Image analysis using edge detection software gave a time series of a cell's shape over the course of the experiment.

The percent stretch was determined by measuring the relative aspect ratios of a cell over time. The aspect ratio is defined as the minor axis divided by the major axis of the trapped cell. By measuring this throughout a cell stretching experiment, the percent stretch, ϵ, was calculated in the following way:

$$\epsilon = 100 \times [(n_x/n_y)_t - (n_x/n_y)_0]/(n_x/n_y)_0,$$

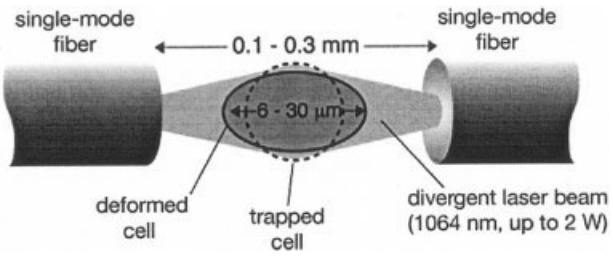

FIG. 2. A cell is stably trapped between two opposing divergent laser beams. At high enough intensities, the cell will be stretched out along the laser axis.

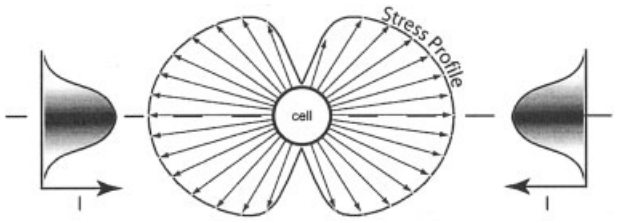

FIG. 3. Stress profile at the surface of a spherical cell trapped by two opposing laser beams with Gaussian profiles. The forces are always normal to the surface, and toward the less optically-dense surrounding medium.

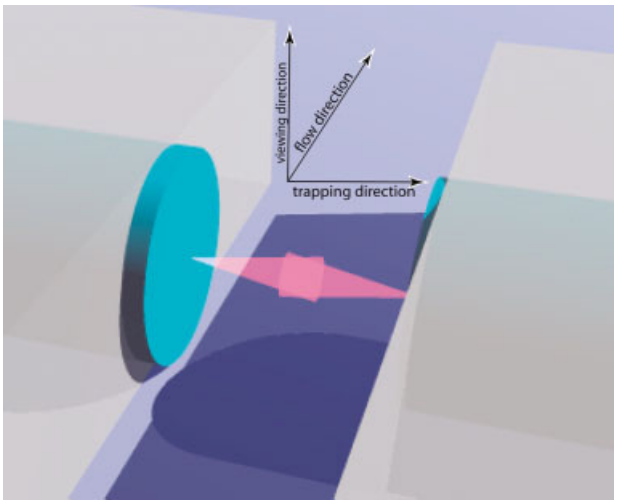

FIG. 4. 3D representation of a generic flow chamber. Design shows several factors: a well controlled flow path, excellent optical alignment of the fibers, and an uninhibited view field. The trapping and stretching region, seen here where the two divergent beams cross, is situated at the center of the flow channel. [Color figure can be viewed in the online issue, which is available at www.interscience.wiley.com].

where n_x and n_y are the cell dimension along and perpendicular to the laser axis, respectively, in units of pixels, while $(n_x/n_y)_0$ is the aspect ratio of the cell at $t < 0.1$ s, and $(n_x/n_y)_t$ is the aspect ratio of the cell at time t.

The aspect ratio was chosen over a simple length measurement in order to minimize errors that could come from slight changes in the cell's position relative to the focal plane from one image to the next.

Variation in cell size was also taken into account. A stress profile was calculated as a function of cell size in an otherwise fixed trapping scenario. By calculating the total stretching force parallel and perpendicular to the beam axis, an aspect stress ratio (i.e., the stress profile along the beam axis divided by the stress profile in the perpendicular direction), was calculated for each cell. A reference aspect stress ratio was then chosen to normalize the calculated percent stretch values, and this one reference value was used for all cell types. The end result is a calculated size corrected percent stretch, ϵ_s, for each cell:

$$\epsilon_s = [A_{\text{ref}}/A_{\text{cell}}]\epsilon,$$

where A_{cell} is the aspect stress ratio (f_x/f_y) for a particular cell, f_x and f_y are the calculated stretching force along the beam and perpendicular to the beam axis, respectively, and A_{ref} is the reference aspect ratio selected for all cells and types (fiducial point).

Cell Lines

Red blood cells were harvested as previously described (3). Polymorphonuclear cells (PMNs) were separated from whole blood using density gradient centrifugation (HISTOPAQUE; Sigma Diagnostics, St. Louis, MO) according to the product information provided.

MCF-10 and MCF-7 cell lines were obtained from the American Type Culture Collection (ATCC) in Rockville, MD. MCF-10 cells are normal, noncancerous mammary epithelial cells that have been immortalized. MCF-7 cells are nonmotile, nonmetastatic epithelial cancer cells. Phorbol ester 12-O-tetradecanoylphorbol-13-acetate (TPA), in the amount of 100 nM, was used to treat MCF-7 cells for 18 h to produce modMCF-7 cells. The action of TPA on MFC-7 cells has been well characterized (28), the result being a significant (18-fold) increase in cellular invasiveness. Each cell type was harvested using trypsin-EDTA and washed and suspended using PBS before being measured in the microfluidic optical stretcher.

RESULTS

A first result was the successful combination of the optical stretcher with a microfluidic delivery system (Fig. 5). This increased throughput leads to better statistics, allowing for the investigation of optical deformability as a very sensitive measure of some of the more subtle changes in a cell's functioning. As a first proof of principle, experiments were performed to measure and compare the optical deformability of two easily distinguished cell types; red blood cells (RBCs) and polymorphonuclear cells (PMNs) (Fig. 6). RBCs were stretched by about 20% at a laser power of 0.086 W from each beam. PMNs were stretched on the order of 5% at about 10 times the power at which the RBCs were quickly torn apart (data not shown). Thus, RBCs, which lack internal structure, have a much higher optical deformability than PMNs, as expected.

After these initial experiments, we wanted to show that we can also distinguish between cells with more subtle differences in their cytoskeleton. For this, we investigated the malignant transformation of human breast epithelial cells, using normal human breast epithelial cells (MCF-10)

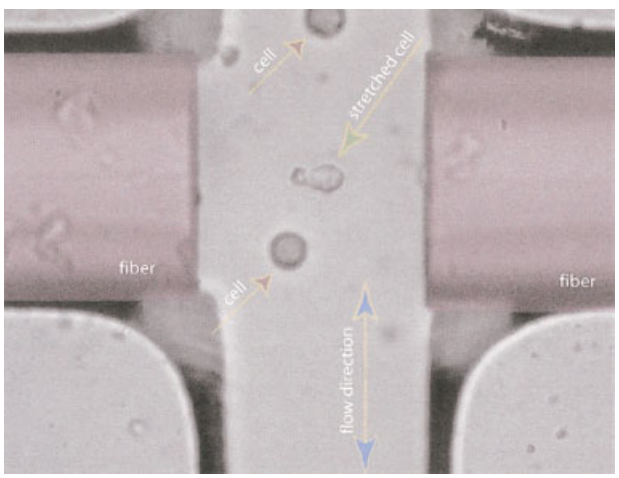

FIG. 5. Cells are flowing in a microfluidic optical stretcher with channels constructed in polydimethylsiloxane (PDMS). One cell has been trapped and stretched out, while two others are being microfluidically transported. [Color figure can be viewed in the online issue, which is available at www.interscience.wiley.com].

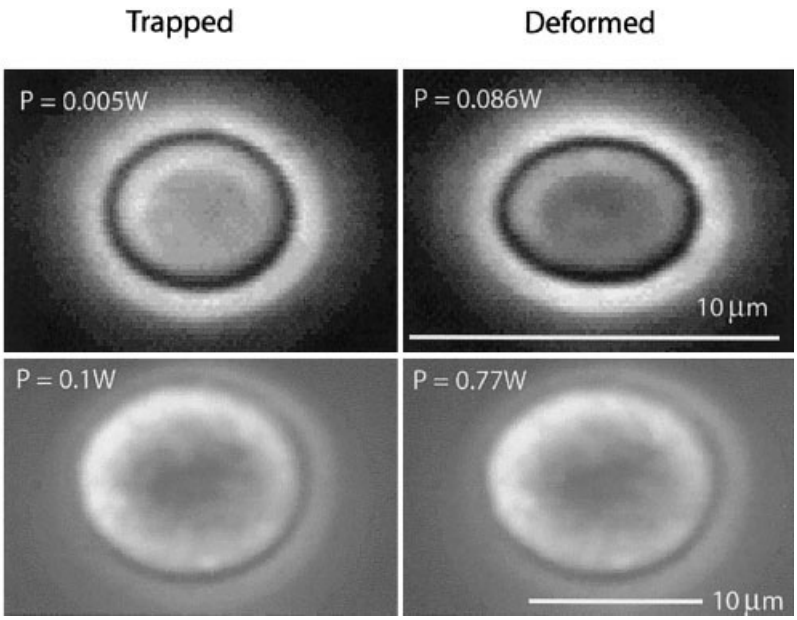

FIG. 6. Deformation of a red blood cell (RBC) and a polymorphonuclear cell (PMN) are shown. The left images show cells at low trapping powers, while the right images show the same cells being stretched at higher laser powers, with values given in each image. The RBC shown here has a percent stretch $\epsilon = 19 \pm 0.5\%$, while the PMN has a mere $\epsilon = 5 \pm 0.3\%$, despite a much higher applied stretching power.

and their cancerous counterparts (MCF-7, modMCF-7). MCF-7 cells are nonmetastatic, while modMCF-7 are created using phorbol esters known to induce metastatic behavior in MCF-7 cells (28).

Plotting the size-corrected percent stretch, ϵ_s, of MCF-10, MCF-7, and modMCF-7 cells shows a clear trimodal distribution with no overlap within one standard error (Fig. 7). A Student's t-test was performed to check that the data sets for these three cell types were distinguishable (data not shown).

Cancer cells (MCF-7) were found to stretch about five times more than normal cells (MCF-10), while metastatically-competent cells (modMCF-7) were found to stretch about twice as much as nonmetastatic cancer cells (MCF-7). Additionally, there was no overlap at all between the normal cells and the metastatically competent cells, indicating a clear cut-off point between the two, as indicated in Figure 7. This was achieved while measuring a mere 83 cells total with rudimentary implementation of flow and automation, which shows that optical deformability is a very good, highly-regulated cell marker.

DISCUSSION

The goal of cytomics is to understand the structure and function of individual cells in relation to their molecular makeup (29). The microfluidic optical stretcher, which utilizes a cell's optical deformability as a cell marker, is a new and powerful tool in this area, as exemplified in the context of cancer diagnostics. While specific molecular markers have more recently been employed to diagnose some cancers, these specific markers are often not present. Rather, cancers are characterized by changes in molecular data patterns that are difficult to utilize directly for fast detection of diseased cells. Here we show that, instead, optical deformability can be used to assess the cumulative effect of these molecular changes as reflected in a cell's elasticity. This can be done in cytological samples obtained by minimally invasive methods (fine-needle aspiration, cytobrushes) (30), which has obvious advantages over traditional methods of cancer diagnosis that

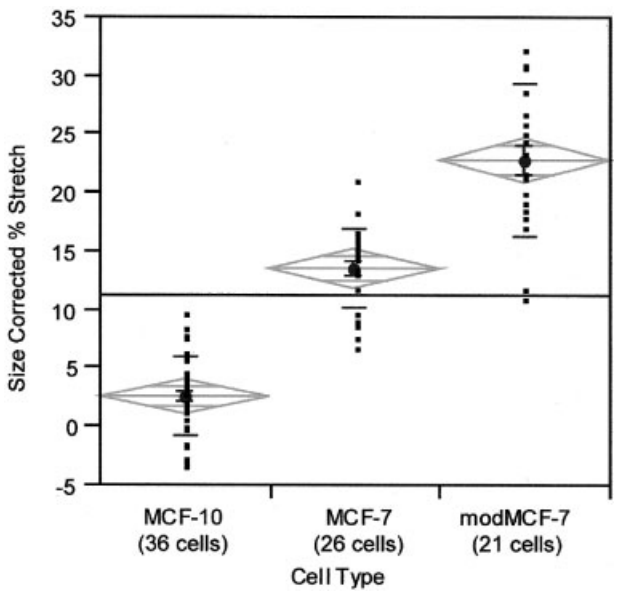

FIG. 7. Optical deformability of normal (MCF-10), cancerous (MCF-7), and metastatically competent cells (modMCF-7). The stretch distribution is represented by a diamond. Its height shows one standard error about the mean percent stretch, while the width shows the relative number of cells of each type. The independent horizontal lines indicate one standard deviation about the mean percent stretch. A line is drawn to show a reasonable cutoff between normal and metastatically competent populations using the size-corrected percent stretch. Exact number measured is given under each cell type.

rely on the optical inspection of histological sections, and in which biopsies are required to obtain a coherent tissue sample. Additionally, cancer can often times not be clearly distinguishable from inflamed tissue (dysplasia) histologically (31). Thus, optical deformability could be seen as a complimentary, and in some cases alternative, method of cancer detection.

Cancer is only one set of examples of disease that can effect changes in the cytoskeleton. There are many other examples that point toward a strong connection between disease and cytoskeletal status: cytoskeletal alterations of blood cells that cause capillary clogs in circulatory problems (32); genetic disorders of intermediate filaments and their cytoskeletal networks that lead to problems with skin, hair, liver, colon, and motor neuron diseases such as amyotrophic lateral sclerosis (ALS) (33); various blood diseases, including sickle-cell anemia, hereditary spherocytosis, or immune hemolytic anemia (34); and the phagocytosis disorders of macrophages suspected to cause certain autoimmune diseases, such as systemic lupus erythematosus (SLE) (35).

While disease is an example of a rather extreme restructuring into a completely new kind of cell, experiments can also aim to investigate structural changes over the life of a single cell type. By synchronizing the cell cycle within a cultured population, the optical deformability of many cells could be measured as they progress toward division. It is known that the cytoskeleton undergoes significant changes during this process, including microtubules separating chromosomes and an actin contractile ring pinching off daughter cells (1); these changes could be monitored with the microfluidic optical stretcher and correlated with known cell-cycle markers such as DNA content. Ultimately, a cell's position in the cell cycle could be determined by optical deformability measurements alone.

Another possibility would be to monitor optical deformability during differentiation. Following this kind of cellular process would be the reverse of studying malignant transformation, with cells developing a more rigid cytoskeleton rather than degrading its structure. This would lead to the distinguishing of stem cells from differentiating cells in much the same way one can discern cancer cells from normal cells.

The next logical step from detecting subpopulations would be to sort them. This would be done microfluidically, and would have the potential for high accuracy. Characterization and sorting of blood cells are an obvious application, because they reside naturally in suspension and are easily accessible. In addition, some blood cell types can be clearly identified by specific surface markers, enabling a measured correlation between their optical deformability and the expression of their surface markers, which can be measured simultaneously on each cell when the microfluidic optical stretcher is mounted on a microscope prepared for fluorescence. This would be an elegant way of confirming the reliability of deformability as a cell marker, and could then be used to gather data on cells that are inaccessible to fluorescence markers. This includes the identification and separation of the 1% hematopoietic stem cells (HSCs) normally circulating in blood. Enriched HSC suspensions are currently used for a large number of novel therapeutic approaches. Optical deformability as an inherent cell marker has several advantages over antibodies tagged with fluorophores or magnetic beads, in that it does not require any specific preparation or labeling, it does not trigger signaling pathways like the binding of antibodies to surface proteins (36), and the cells remain immaculate. This is important for therapeutic applications because cells contaminated with fluorescent dyes or magnetic particles could not be used in humans.

Using step-stress experiments, the cells' immediate elastic response (normalized by the size-corrected stress), currently defined as optical deformability, has been sufficient to distinguish cells. It is, however, only one of several parameters that can be measured. Because cells are viscoelastic, the multidimensional phase space is spanned by magnitude and duration (or frequency) of applied stress as well as magnitude and time- (or phase-) dependence of the observed deformation. In one or more of these dimensions, the cells will most likely differ. This kind of experimental flexibility, along with high throughput, allows for a wide range of investigations involving variation of cellular structure.

In conclusion, the microfluidic optical stretcher is a new tool that can probe a cell's deformability with a resolution capable of diagnosing diseases and identifying cells based on cytoskeletal changes, which are involved in many cellular functions. A comparison can be drawn with early flow cytometry, some 25 years ago, when advances were first being made on the road from measuring a few fluorescent cells on a glass slide toward the current ability to measure the fluorescence of hundreds of thousands of cells per minute. With proper technological improvement, including automation and parallelization, measuring the deformability of several thousand cells per minute now seems possible. The microfluidic optical stretcher faces its own challenges en route to a similar end, but the result would be a completely noninvasive, non–marker-specific alternative to current cytometry, which would be a valuable tool for the human cytome project.

ACKNOWLEGMENTS

We thank Josef Käs and Revathi Ananthakrishnan for their continued support.

LITERATURE CITED

1. Ibrahim SF, van den Engh G. High-speed cell sorting: fundamentals and recent advances. Curr Opin Biotechnol 2003;14:5–12.
2. Guck J, Ananthakrishnan R, Moon TJ, Cunningham CC, Käs J. Optical deformability of soft biological dielectrics. Phys Rev Lett 2000;84: 5451–5454.
3. Guck J, Ananthakrishnan R, Mahmood H, Moon TJ, Cunningham CC, Käs J. The optical stretcher: a novel laser tool to micromanipulate cells. Biophys J 2001;81:767–784.
4. Alberts B, Johnson A, Lewis J, Raff M, Roberts K, Walter P. Molecular biology of the cell. New York: Garland Publishing;1994. p. 907–981.
5. Janmey PA, Euteneuer U, Traub P, Schliwa M. Viscoelastic properties of vimentin compared with other filamentous biopolymer networks. J Cell Biol 1991;113:155–160.
6. Wang N, Stamenovic D. Contribution if intermediate filaments to cell

stiffness, stiffening and growth. Am J Physiol Cell Physiol 2000;279: C188–C194.
7. Wang N, Butler JP, Ingberg DE. Mechanotransduction across the cell surface and through the cytoskeleton. Science 1993;260:1124–1127.
8. Jamora C, Fuchs E. Intercellular adhesion, signaling and the cytoskeleton. Nat Cell Biol 2002;4:101–108.
9. Rao KMK, Cohen HJ. Actin cytoskeletal network in aging and cancer. Mutat Res 1991;256:139–148.
10. Cunningham CC, Gorlin JB, Kwiatkowski DJ, Hartwig JH, Janmey PA, Byers HR, Stossel TP. Actin-binding protein requirement for cortical stability and efficient locomotion. Science 1992;255:325–327.
11. Moustakas A, Stournaras Ch. Regulation of actin organisation by TGF-beta in H-ras-transformed fibroblasts. J Cell Sci 1999;112:1169–1179.
12. Hall A. Rho GTPases and the actin cytoskeleton. Science 1998; 279: 509–514.
13. Erzurum SC, Kus ML, Bohse C, Elson EL, Worthen GS. Mechanical properties of HL60 cells: role of stimulation and differentiation in retention in capillary-sized pores. Am J Respir Cell Mol Biol 1991;5: 230–241.
14. Olins A, Herrmann H, Lichter P, Olins DE. Retinoic acid differentiation of HL-60 cells promotes cytoskeletal polarization. Cell Res 2000; 254:130–142.
15. Hochmuth RM. Micropipette aspiration of living cells. J Biomech 2000;33:15–22.
16. Ward KA, Li W, Zimmer S, Davis T. Viscoelastic properties of transformed cells: role in tumor cell progression and metastasis formation. Biorheology 1991;28:301–313.
17. Mahaffy RE, Shih CK, MacKintosh FC, Käs J. Scanning probe-based frequency-dependent microrheology of polymer gels and biological cells. Phys Rev Lett 2000;85:880–883.
18. Rotsch C, Radmacher M. Drug-induced changes of cytoskeletal structure and mechanics in fibroblasts: an atomic force microscopy study. Biophys J 2000;78:520–535.
19. Lekka M, Laidler P, Gil D, Lekki J, Stachura Z, Hrynkiewicz AZ. Elasticity of normal and cancerous human bladder cells studied by scanning force microscopy. Eur Biophys J 1999;28:312–316.
20. Zahalak GI, McConnaughey WB, Elson EL. Determination of cellular mechanical properties by cell poking, with an application to leukocytes. J Biomech Eng 1990;112:283–294.
21. Thoumine O, Ott A. Comparison of the mechanical properties of normal and transformed fibroblasts. Biorheology 1997;34:309–326.
22. Yamada S, Wirtz D, Kuo SC. Mechanics of living cells measured by laser tracking microrheology. Biophys J 2000;78:1736–1747.
23. Sleep J, Wilson D, Simmons R, Gratzer W. Elasticity of the red cell membrane and its relation to hemolytic disorders: an optical tweezers study. Biophys J 1999;77:3085–3095.
24. Eichinger L, Koppel B, Noegel AA, Schleicher M, Schliwa M, Weijer K, Witke W, Janmey PA. Mechanical perturbation elicits a phenotypic difference between dictyostelium wild-type cells and cytoskeletal mutants. Biophys J 1996;70:1054–1060.
25. Johnson RM. Ektacytometry of red cells. Subcell Biochem 1994;23: 161–203.
26. Ashkin A. Acceleration and trapping of particles by radiation pressure. Phys Rev Lett 1970;24:156–159.
27. Guck J, Ananthakrishnan R, Cunningham CC, Käs J. Stretching biological cells with light. J Phys Condens Matter 2002;14:4843–4856.
28. Johnson MD, Torri JA, Lippman ME, Dickson, RB. Regulation of motility and protease expression in PKC-mediated induction of MCF-7 breast cancer cell invasiveness. Exp Cell Res 1999,247:105–113.
29. Valet G, Leary JF, Tárnok A. Cytomics—new technologies: towards a human cytome project. Cytometry 2004;59A:000–000.
30. Dunphy CH, Ramos R. Combining fine-needle aspiration and flow cytometric immunophenotyping in evaluation of nodal and extranodal sites for possible lymphoma: a retrospective review. Diagn Cytopathol 1997;16:200–206.
31. Reibel J. Prognosis of oral pre-malignant lesions: significance of clinical, histopathological, and molecular biological characteristics. Crit Rev Oral Biol Med 2003,14:47–62.
32. Worthen GS, Schwab B 3rd, Elson EL, Downey GP. Mechanics of stimulated neutrophils: cell stiffening induces retention in capillaries. Science 1989;245:183–186.
33. Fuchs E, Cleveland DW. A structural scaffolding of intermediate filaments in health and disease. Science 1998;279:514–519.
34. Bosch FH, Were JM, Schipper L, Roerdinkholder-Stoelwinder B, Huls T, Willekens FL, Wichers G, Halie MR. Determinants of red blood cell deformability in relation to cell age. Eur J Haematol 1994;52:35–41.
35. Bijl M, Limburg PC, Kallenberg CGM. New insights into the pathogenesis of systemic lupus erythematosus (SLE): the role of apoptosis. Neth J Med 2001;59:66–75.
36. Guo Y, Lübbert M, Engelhardt M. CD34(–) hematopoietic stem cells: current concepts and controversies. Stem Cells 2003;21:15–20.